Available online at www.sciencedirect.com
ScienceDirect
Ore Geology Reviews 29 (2006) 307–324
ORE GEOLOGY REVIEWS
www.elsevier.com/locate/oregeorev

Molybdenite Re–Os and albite $^{40}Ar/^{39}Ar$ dating of Cu–Au–Mo and magnetite porphyry systems in the Yangtze River valley and metallogenic implications

Jingwen Mao [a,b,*], Yitian Wang [b], Bernd Lehmann [c], Jinjie Yu [b], Andao Du [b], Yanxiong Mei [b], Yongfeng Li [a], Wenshuan Zang [a], Holly J. Stein [d], Taofa Zhou [e]

[a] *Faculty of Geosciences and Resources, China University of Geosciences, Beijing 100083, People's Republic of China*
[b] *Institute of Mineral Resources, Chinese Academy of Geological Sciences, Beijing 100037, People's Republic of China*
[c] *Institute of Mineralogy and Mineral Resources, Technical University of Clausthal, 38678 Clausthal-Zellerfeld, Germany*
[d] *AIRIE Program, Department of Earth Resources, Colorado State University, Fort Collins, CO 80523-1482, United States of America*
[e] *School of Resources and Environment Engineering, Hefei University of Technology, Hefei 230009, People's Republic of China*

Received 20 May 2004; accepted 7 November 2005
Available online 3 February 2006

Abstract

The area of the Middle–Lower Yangtze River valley, Eastern China, extending from Wuhan (Hubei province) to western Zhenjiang (Jiangsu province), hosts an important belt of Cu–Au–Mo and Fe deposits. There are two styles of mineralization, i.e., skarn/porphyry/stratabound Cu–Au–Mo–(Fe) deposits and magnetite porphyry deposits in several NNE-trending Cretaceous fault-bound volcanic basins. The origin of both deposit systems is much debated. We dated 11 molybdenite samples from five skarn/porphyry Cu–Au–Mo deposits and 5 molybdenite samples from the Datuanshan stratabound Cu–Au–Mo deposit by ICP-MS Re–Os isotope analysis. Nine samples from the same set were additionally analyzed by NTIMS on Re–Os. Results from the two methods are almost identical. The Re–Os model ages of 16 molybdenite samples range from 134.7 ± 2.3 to 143.7 ± 1.6 Ma (2σ). The model ages of the five samples from the Datuanshan stratabound deposit vary from 138.0 ± 3.2 to 140.8 ± 2.0 Ma, with a mean of 139.3 ± 2.6 Ma; their isochron age is 139.1 ± 2.7 Ma with an initial Os ratio of 0.7 ± 8.1 (MSWD = 0.29). These data indicate that the porphyry/skarn systems and the stratabound deposits have the same age and suggest an origin within the same metallogenic system. Albite $^{40}Ar/^{39}Ar$ dating of the magnetite porphyry deposits indicates that they formed at 123 to 125 Ma, i.e., 10–20 Ma later. Both mineralization styles characterize transitional geodynamic regimes, i.e., the period around 140 Ma when the main NS-trending compressional regime changed to an EW-trending lithospheric extensional regime, and the period of 125–115 Ma of dramatic EW-trending lithospheric extension.

Keywords: Re–Os isotopic dating; Ar–Ar dating; Porphyry/skarn/stratabound Cu–Au–Mo deposits; Magnetite porphyry deposits; Middle–Lower Yangtze River metallogenic belt; China

1. Introduction

The Middle–Lower Yangtze River valley is an important Cu–Mo–Au–Fe metallogenic belt in Eastern China. Mining activity can be traced back as far as the

* Corresponding author. Faculty of Geosciences and Resources, China University of Geosciences, Beijing 100083, People's Republic of China. Tel.: +86 10 6832 7333; fax: +86 10 6832 7142.
E-mail address: jingwenmao@263.net (J. Mao).

0169-1368/$ - see front matter © 2005 Elsevier B.V. All rights reserved.
doi:10.1016/j.oregeorev.2005.11.001

Bronze Age and more than 200 Cu–Au–Mo–Fe deposits have been discovered so far. Most of these are concentrated in several areas (ore districts), such as Edong, Jiujiang-Ruicang (or Jiurui), Anqing-Guichi, Tongling, Luzong, Ningwu, and Ningzhen, from west to east along the Middle–Lower Yangtze River valley (Fig. 1). Modern exploration was initially focused on skarn-type Cu- and Fe-deposits following up the ancient remains of mining activities. These deposits were considered to be typical granitoid-related skarn-hydrothermal deposits (W.K. Guo, 1957; Z.S. Guo, 1957; Guo, 1963; Zhao et al., 1990). During the late 1980s and early 1990s, gold was discovered in the gossans of the Cu–Mo deposits (Liu et al., 1988) and some Au-only skarn deposits have been explored, for example, the Jilongshan deposit in the Edong ore district, Hubei province (Zhao et al., 1999). Several dozen subvolcanic Fe deposits were discovered and explored during the 1970s in the Ningwu-Luzhong basins (Fig. 1) (Ningwu Research Group, 1978). The origin of these various styles of mineralization has been much discussed in the Chinese literature and both magmatic-hydrothermal models (Guo, 1982; Hu et al., 1979; Liu et al., 1988; Huang and Chu, 1993; Tang et al., 1998; Zhang et al., 2001; Du et al., 2003; Wu et al., 2003), as well as synsedimentary-exhalative models (Fu, 1977; Gu, 1984; Gu and Xu, 1986; Ji and Wang, 1990; Yue et al., 1993; Pan and Dong, 1999) have been proposed.

Geochronology allows these metallogenic models to be better constrained. There are many K–Ar and Rb–Sr age data from this area, and they define a wide range of 170 to 90 Ma for felsic magmatism and hydrothermal activity in the Middle–Lower Yangtze River valley (Tang et al., 1998). Re–Os and Ar–Ar methods, however, are particularly suitable to date the mineralization and associated hydrothermally altered rocks. In this contribution, we present molybdenite Re–Os ages on Cu–Au–Mo ore samples and ^{40}Ar–^{39}Ar ages on albite from some magnetite porphyry deposits. This data allows us to discuss the metallogenic processes in a geodynamic framework.

2. Geological setting

The Middle–Lower Yangtze River valley metallogenic belt is located on the northern margin of the Yangtze craton, south of the North China craton and

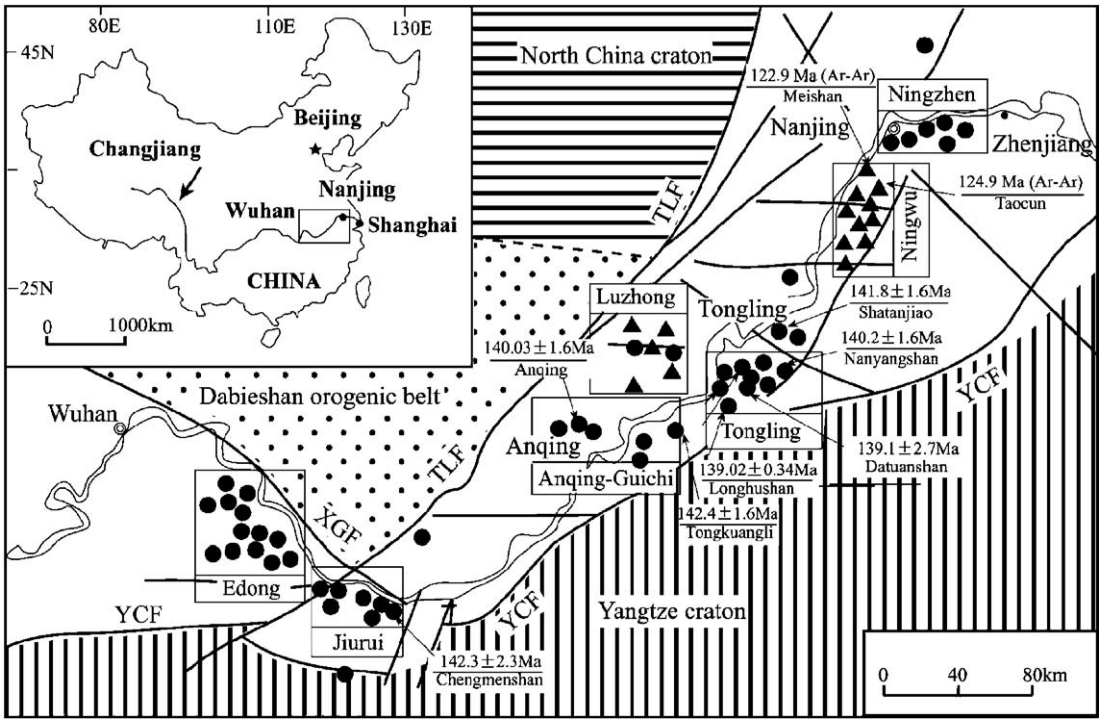

Fig. 1. Distribution of metallic deposits and their ages in the Middle–Lower Yangtze River belt, based on the map of Pan and Dong (1999). Except for the Ar–Ar dating labeled, all other data by Re–Os model or isochron method. The age date for Longhushan is taken from Sun et al. (2003); all others were obtained in this study. Explanation: circle: porphyry–skarn–stratabound Cu–Au–Mo deposits; triangle: magnetite porphyry deposits. YCF—Yangxing-Changzhou fault, XGF—Xiangfan-Guangji fault, TLF—Tancheng-Lujiang fault. White area is the Middle–Lower Yangtze River belt.

Qinling-Dabie orogenic belt. Several large strike-slip fault systems characterize the border zone of the Yangtze and North China cratons (Fig. 1). Yanshanian (Jurassic–Cretaceous) magmatism and related Cu–Au–Mo–Fe deposits developed at fault intersects (Zhai, 1992; Wu and Wu, 1999).

The stratigraphic sequence in the Middle–Lower Yangtze valley is composed of three tectonostratigraphic units, i.e., Pre-Sinian metamorphic basement, Sinian to Early Triassic submarine sedimentary cover, and Middle Triassic to Cretaceous terrestrial clastic and volcanic rocks. The Pre-Sinian metamorphic rocks consist of gneiss, schist, phyllite, and slate, and are found scattered throughout the valley. Sinian conglomerate, tillite, dolomites, shale, and chert discordantly overlie the Pre-Sinian metamorphic rocks. Cambrian and Ordovician siltstone and shale intercalated with dolomitic limestone and marl conformably overlie Sinian clastic rocks and dolomite. Silurian strata are characterized by thick quartz sandstone, arkose intercalated with shale, marl, and dolomite. From Late Silurian to Devonian, the valley was uplifted and had a positive relief. Late Devonian terrestrial clastic rocks consist of thick layers of quartz sandstone, sandstone and basal conglomerate, coal seams and hematite layers. Carboniferous littoral-facies carbonate rock conformably overlies the Late Devonian clastic rocks. Permian sedimentary rocks, extensively distributed throughout the whole belt, are composed of littoral to shallow marine facies carbonates, intercalated with carbonaceous shale in the upper part, and interbedded marine and terrestrial facies carbonates intercalated with some silicic, marl, Ca-rich shale, sandstone, siltstone and coal-bearing sedimentary rocks in the lower part (Zhai et al., 1992). The Lower Triassic sedimentary rocks are shallow marine to littoral dolomites, limestone and minor gypsum, and are widely distributed throughout the entire belt. The Middle Triassic is characterized by interbedded marine dolomite, marl, limestone and terrestrial marl, siltstone. The Upper Triassic is terrestrial argillaceous siltstone, fine-grained sandstone with coal seams and locally sandstone copper mineralization. From the Jurassic to Cretaceous, a series of terrestrial fault-bound basins developed along the Middle–Lower Yangtze River valley. The Jurassic system consists of lake- and swamp-facies sandstone, siltstone, shale, and a layer of volcanoclastic rocks on top. The Lower and Middle Cretaceous consist mainly of volcanic rocks and volcanoclastic rocks comprising andesite, rhyolite, shoshonite, trachyte, trachytic basalt, basaltic andesite, welded breccia and tuff. The Upper Cretaceous is characterized by red-bed sedimentary clastic rocks: conglomerate, sandy conglomerate, sandstone and siltstone intercalated with minor andesite, basalt and thin layers of gypsum. Tertiary strata comprise conglomerate, sandstone, basaltic tuffaceous breccia, lava and agglomerate.

There is extensive Cretaceous felsic magmatism. Three types of Mesozoic granitoids have been recognized: (1) high-K calc-alkaline granodiorite series related to Cu–Au–Mo–(Fe) polymetallic mineralization, comprising gabbro, diorite, quartz diorite, and granodiorite, which belong to I-type (Pei and Hong, 1995) or magnetite-type granitoids (Ishihara, 1977). According to Wu et al. (1996), their $^{40}Ar/^{39}Ar$ age is 139.8 to 135.8 Ma. The initial $^{87}Sr/^{86}Sr$ ratios of the plutonic rocks range from 0.7040 to 0.7087 and their REE distribution patterns are LREE-enriched and dip to the right (Zhao et al., 1999). In light of high Sr and low Y abundances, Zhang et al. (2001) and Wang et al. (2001) proposed that this suite of granitoids is adakitic, and inferred that they are products of partial melting of young underplating basic granulite of Mesozoic age beneath the lower crust of North China. (2) The Na-rich calc-alkaline diorite series consists of pyroxene diorite porphyry, diorite porphyry, and their corresponding eruptive rocks, which were termed as shoshonite series by Wang et al. (1996). The volcanic rocks occur in five Late Mesozoic subaerial basins (from west to east, the Jinbao-Huaining basins of the Edong ore district, the Luzong basin of the Luzong district, and the Fanchang and Ningwu basins of the Ningwu district), with a total area of about 5000 km^2 (Pan and Dong, 1999). Zhang et al. (2003) dated them at 127 to 131 Ma using SHRIMP zircon U–Pb methods. (3) The A-type granitoids consist of quartz syenite, syenite, quartz monzonite, alkaline granite, and their corresponding eruptive rocks are phonolite. The latter were dated at 110 to 97 Ma by Tang et al. (1998). At present, there are no ore deposits known to be related to them.

There are two types of mineralization in the Middle–Lower Yangtze River valley, i.e., porphyry/skarn/stratabound Cu–Au–Mo–(Fe) deposits and magnetite porphyry deposits related to andesitic rocks. The former are mainly developed around the Mesozoic granitoid intrusions and are hosted in both the intrusions, as well as the Carboniferous, Permian and Triassic carbonate host rocks. In the past 10 years, several skarn Au–(Cu) (Zhao et al., 1999) and porphyry Au-only deposits have been explored in the belt. These are members of the porphyry/skarn/stratabound Cu–Au–Mo–(Fe) deposit spectrum. Gold mineralization has

also been discovered outside the stratabound Cu–Au–Mo–(Fe) deposits, in a situation similar to the metal zoning in the Bingham porphyry Cu (Au) ore district.

The porphyry iron mineralization occurs in massive and disseminated ores in roof pendants (or cupolas) of the porphyry stocks, and in lodes in the volcanic

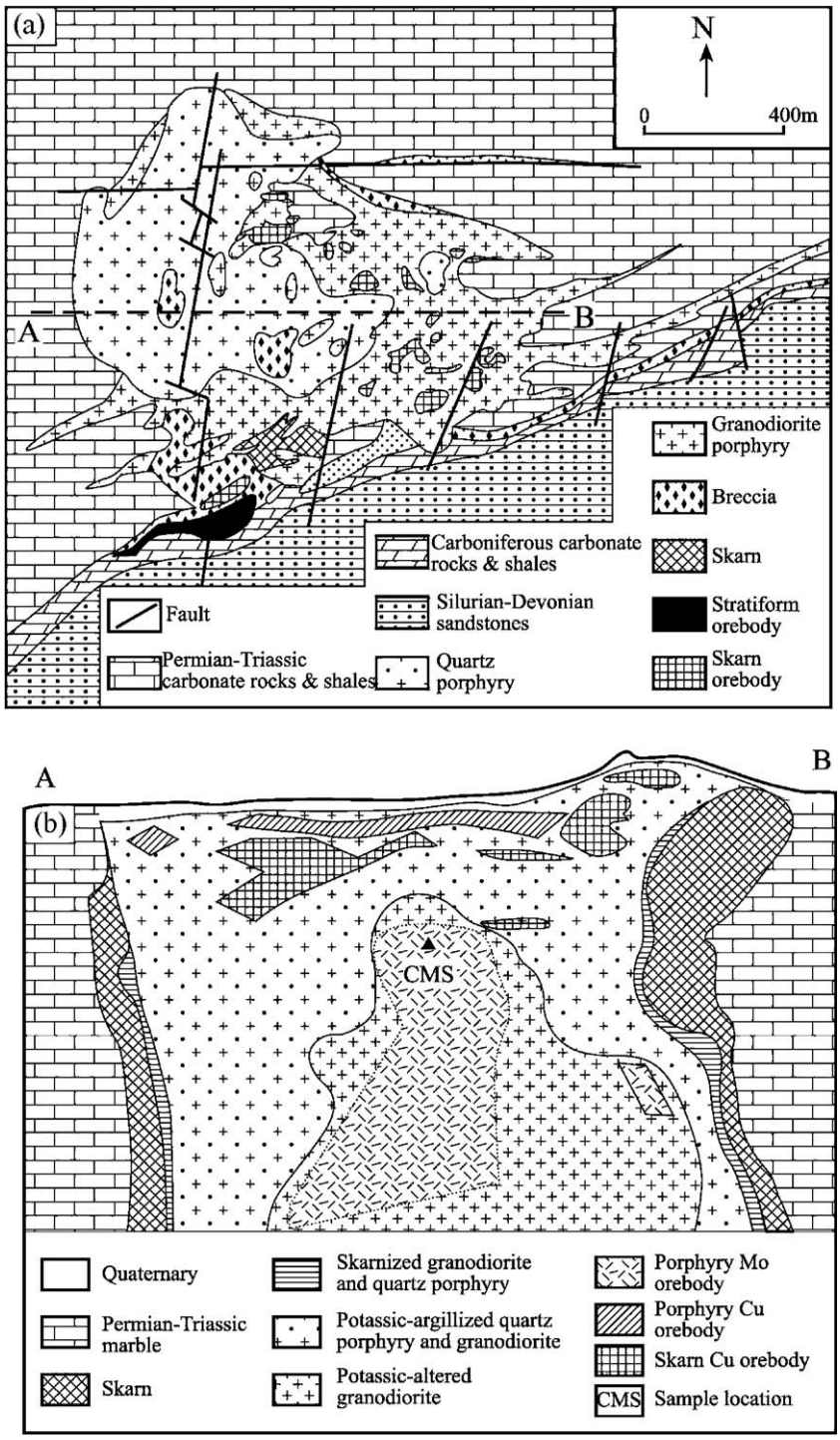

Fig. 2. Geology of the Chengmenshan porphyry/skarn Cu–Mo deposit and sample locations in the Jiurui ore district, Jiangxi province: (a) geological map; (b) cross-section with sample location (modified from Zhai et al., 1992).

host rocks, and is accompanied by strong albite alteration with the assemblage albite–(or marialite)–actinolite (or diopside)–apatite.

3. Sampling

Sixteen molybdenite samples were collected from six Cu–Au–Mo or Cu–Mo deposits, i.e., the Chengmenshan Cu–Mo deposit (Jiurui area), the Anqing Cu–Mo and Tongkuangli Mo deposits (Anqing-Guichi area), and the Datuanshan, Nanyangshan and Shatanjiao Cu–Mo deposits (Tongling area).

The Chengmenshan deposit is situated in the east of the Jiurui area. It consists of porphyry Cu and Mo orebodies, skarn and stratabound Cu–Au orebodies (Pan and Dong, 1999). The deposit was discovered in the 1980s and has been mined in an open pit since 2002. The host rocks for the mineralization include both granodiorite and Permian–Triassic carbonate rocks. The Yanshanian granitoid stock at the Chenmenshan mine has an outcrop area of only 0.8 km^2 at surface. A K–Ar biotite age of 142 to 153 Ma for the main granodiorite porphyry body and a whole-rock K–Ar age of 118 to 120 Ma for the central quartz porphyry have been obtained (Huang and Chu, 1993; Ji and Wang, 1990). The mineralization occurs in roof pendants of the granodiorite stock and the proximal contact with the Permian–Triassic carbonate rocks. The deposit has an indicated reserve of 3.07 Mt Cu with average grade of 0.75%, 43.6 t Au with average grade of 0.24 g/t, and a Mo grade of 0.047%. Many breccia pipes developed within and surrounding the granitoid stock (Fig. 2a). The dominant alteration consists of K-feldspar alteration, silicification, argillization, skarn and sericitization. The molybdenite samples we have analyzed are taken from the porphyry Mo orebodies at the roof pendant of the Chengmenshan granodiorite stock (Fig. 2b).

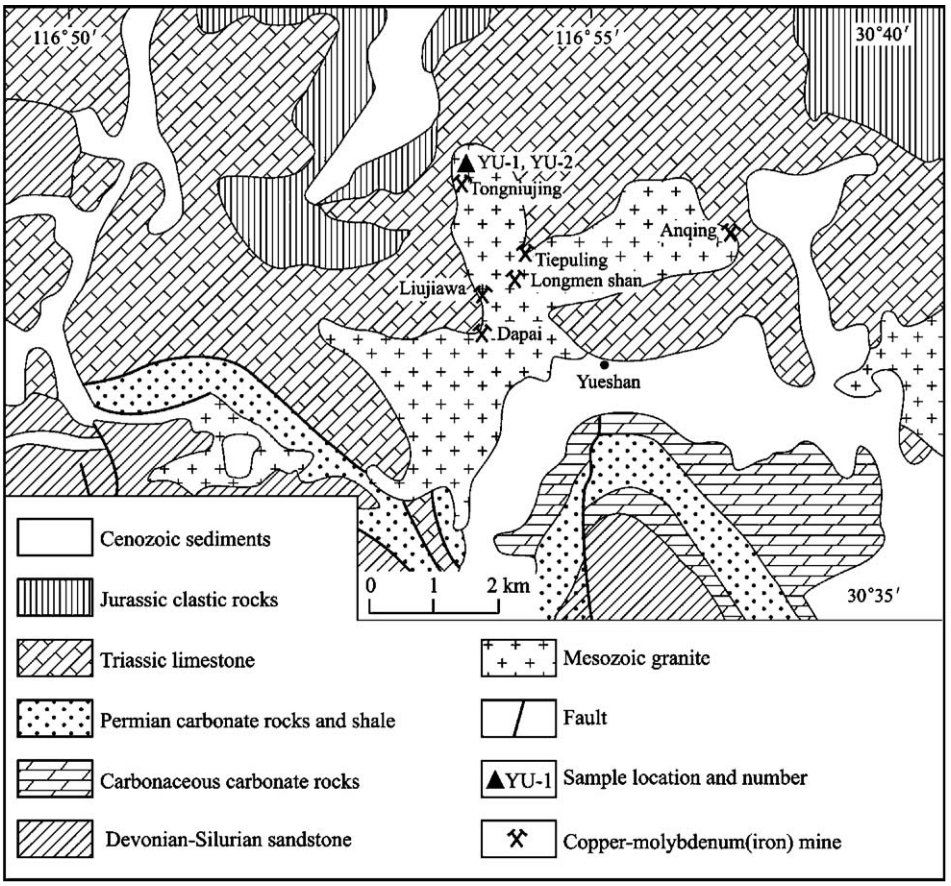

Fig. 3. Simplified geology and sampling location in the Yueshan Cu–Au–Mo–Fe ore district, Anqing-Guichi area in Anhui province (modified from Sun et al., 2003). The Yueshan ore district consists of the Tongniujing, Anqing, Longmenshan, Liujiawa, Tiepuling Cu–Au–Mo–Fe deposits and Dapai iron deposit located at the contacts of the Yueshan Mesozoic granitoid stock. The samples YU-1 and YU-2 are taken from the small open pit of the Tongniujing mine, north contact of the Yueshan granitoid stock.

The Yueshan Cu–Au–Mo–(Fe) ore district is the most important one in the Anqing-Guichi area, which includes Tongniujing, Anqing, Longmenshan, Liujiawa, Tiepuling Cu–Au–Mo–Fe deposits and Dapai iron deposit (Fig. 3). These deposits occur in the endo- and exocontact zones of the Yueshan Mesozoic granitic stock and the carbonate rocks. The Yueshan granitoid stock consists of diorite, granodiorite and quartz diorite (Zhou et al., 2002), and the host rocks for both Cu–Mo–Fe orebodies and granitic stock are the Triassic carbonate rocks (Fig. 3). There are skarn Cu–Fe, skarn Au, skarn Fe, and hydrothermal vein-stockwork Cu–Mo–Au mineralizations in the ore field. We collected two molybdenite samples from the stockwork orebody in a small open pit in the Tongniujing mine (Fig. 3).

The Tongkuangli deposit, a small skarn-hydrothermal Mo deposit, located in the easternmost part of the Anqing-Guichi area, is the only deposit hosted in Cambro-Ordovician carbonate rocks in the metallogenic belt. There is a small outcrop of granite at the surface, but the geophysical survey indicates that it is getting large beneath the mine area (Tang et al., 1998). The Mo mineralization occurs in multiple layers (Fig. 4), hosted within calcic skarn consisting of diopside, garnet and vesuvianite and wollastonite, and resulting from replacement of the marl and the lime-rich pelite. Local farmers are currently mining this deposit, and we collected some ore samples from the ore heap. Striped molybdenite superimposed on skarnified marble can be seen.

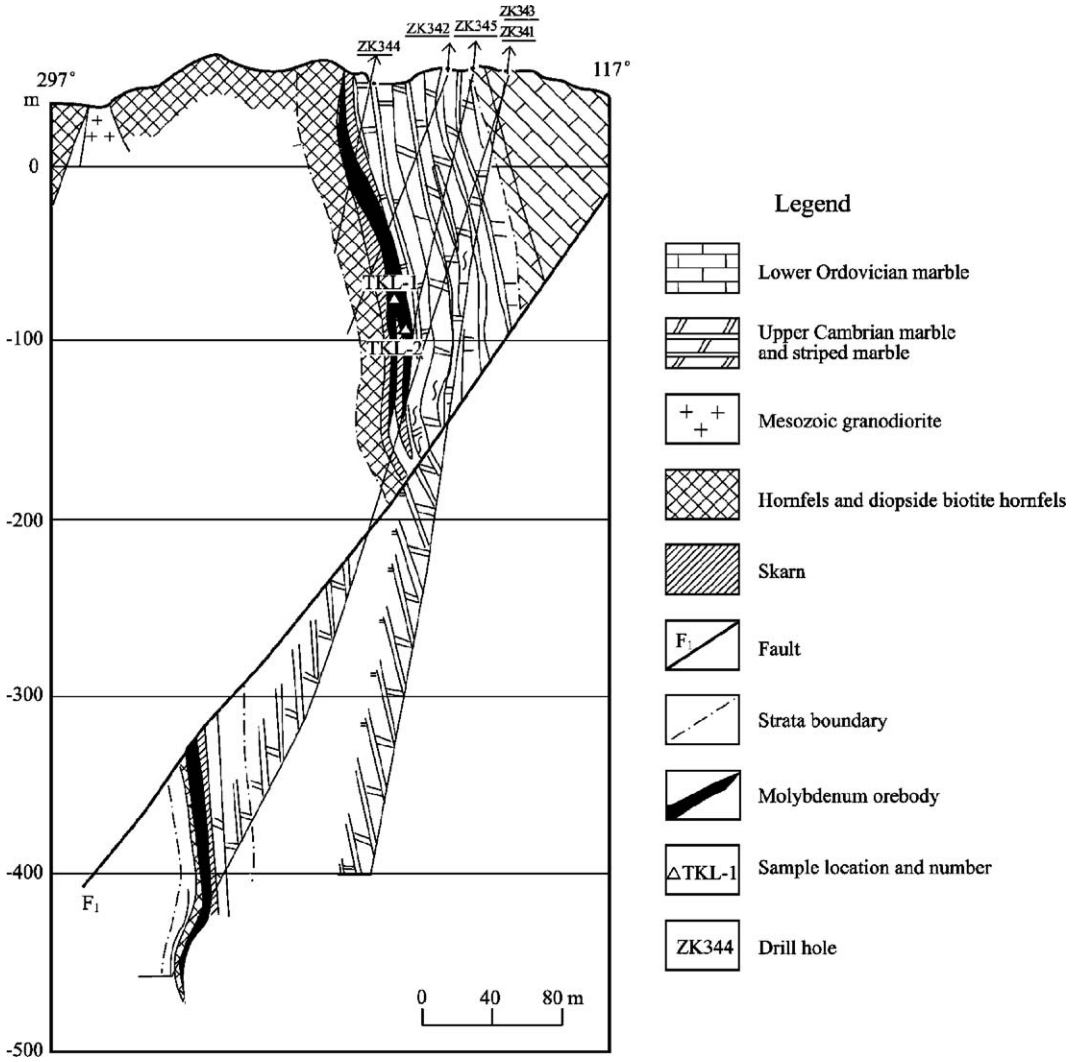

Fig. 4. Geological section and sample location for the Tongkuangli molybdenum deposit in the Anqing-Guichi area in Anhui province. The molybdenum orebody is hosted by Upper Cambrian carbonate rocks, which were metasomatized to skarn and hornfels.

The Datuanshan deposit is one of the largest Cu deposits in the Tongling area, the largest one in the Middle–Lower Yangtze River metallogenic belt. In the ore deposit, all the orebodies are distributed in strata-like shape around the Mesozoic granitic dikes (Fig. 5). The host rocks for both the Cu–Au–Mo orebodies and the granitic dikes are Triassic–Permian carbonate rocks. The mineralization is especially well developed at the boundary between the Triassic and Permian strata, where the stratabound orebody is thicker than usual. Sulfides (chalcopyrite, pyrrhotite, pyrite and molybdenite), are superimposed on the calcic skarn intercalated with hornfels. We collected five samples from cores of drillholes ZK231 and ZK3815 that intersect the Mo orebody (Fig. 5).

Nanyangshan and Shatanjiao, two small-scale skarn Cu–Mo deposits, are situated on the southeastern contact zone of the Xinwuli granodiorite intrusion and the southern contact zone of the Shatanjiao granodiorite intrusion, respectively. They are mined by the local farmers, and our samples derive from ore heaps. Both deposits are typical skarns, with development of both skarn and retrograde alteration. Molybdenite is intergrown with pyrite; chlorite and actinolite are superimposed on the garnet–pyroxene–epidote–vesuvianite skarn.

The NNE-striking Cretaceous basin of Ningwu has three areas with dense distribution of magnetite porphyry deposits (Fig. 6); the Meishan deposit in the north, Washan in the center, and the Zhonggu deposit in the south. The Cretaceous volcanic belt in the basin is 3 to 16 km in width and consists of andesitic volcanic clastic rocks, tuff, lava of the Longwangshan Formation; andesitic volcanic rocks, tuff, and lava of the Dawangshan Formation; andesitic tuff and lava of the Gushan Formation; and andesitic volcanic rocks, tuff, and lava of the Niangniangshan Formation, which represent four cycles of volcanic eruption. A great number of Cretaceous volcanic rock-related pyroxene diorite and diorite stocks occur beneath the centers of the volcanic eruption, where magnetite porphyry deposits developed within stockworks hosted in volcanic rocks. This suite of volcanic rocks discordantly overlies on Jurassic clastic rocks intercalated with some andesitic tuff and breccia, as well as several thin coal seams, and on Triassic carbonate and clastic rocks intercalated with a thin coal seam. In the peripheral margin of the basin, the volcanic suite overlies Devonian carbonate rocks. The volcanic suite is discordantly overlain by Upper Cretaceous red-bed lake-facies clastic rocks intercalated with some gypsum layers, and Tertiary fine-grained sandstone, conglomerate and basalt and olivine-bearing basalt, as well as Quaternary gravel, sand and clay deposits. The magnetite porphyry deposits are accompanied by strong alteration zoning, i.e., a diopside–

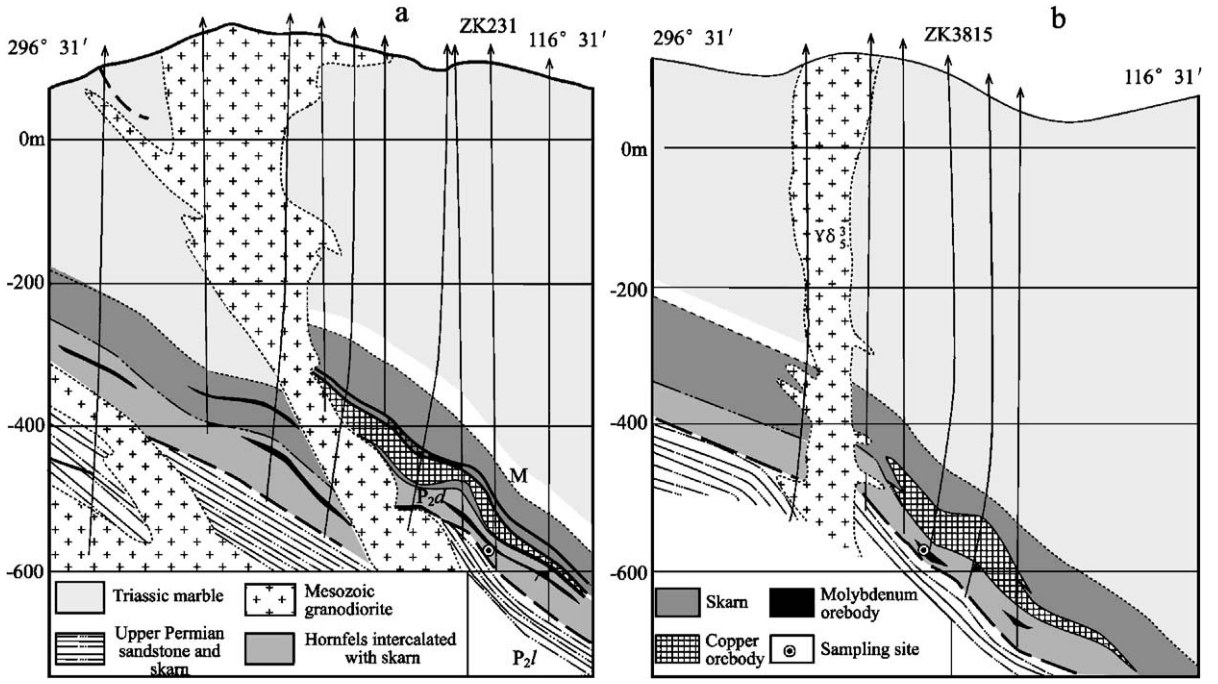

Fig. 5. Geological sections of No. 23 (a) and No. 38 (b) exploration lines of the Datuanshan Cu–Mo–Au deposit with sampling locations labeled (modified from Mei et al., 2005). We took the samples from the molybdenum ore-layer beneath the copper ore-layer from the drill holes.

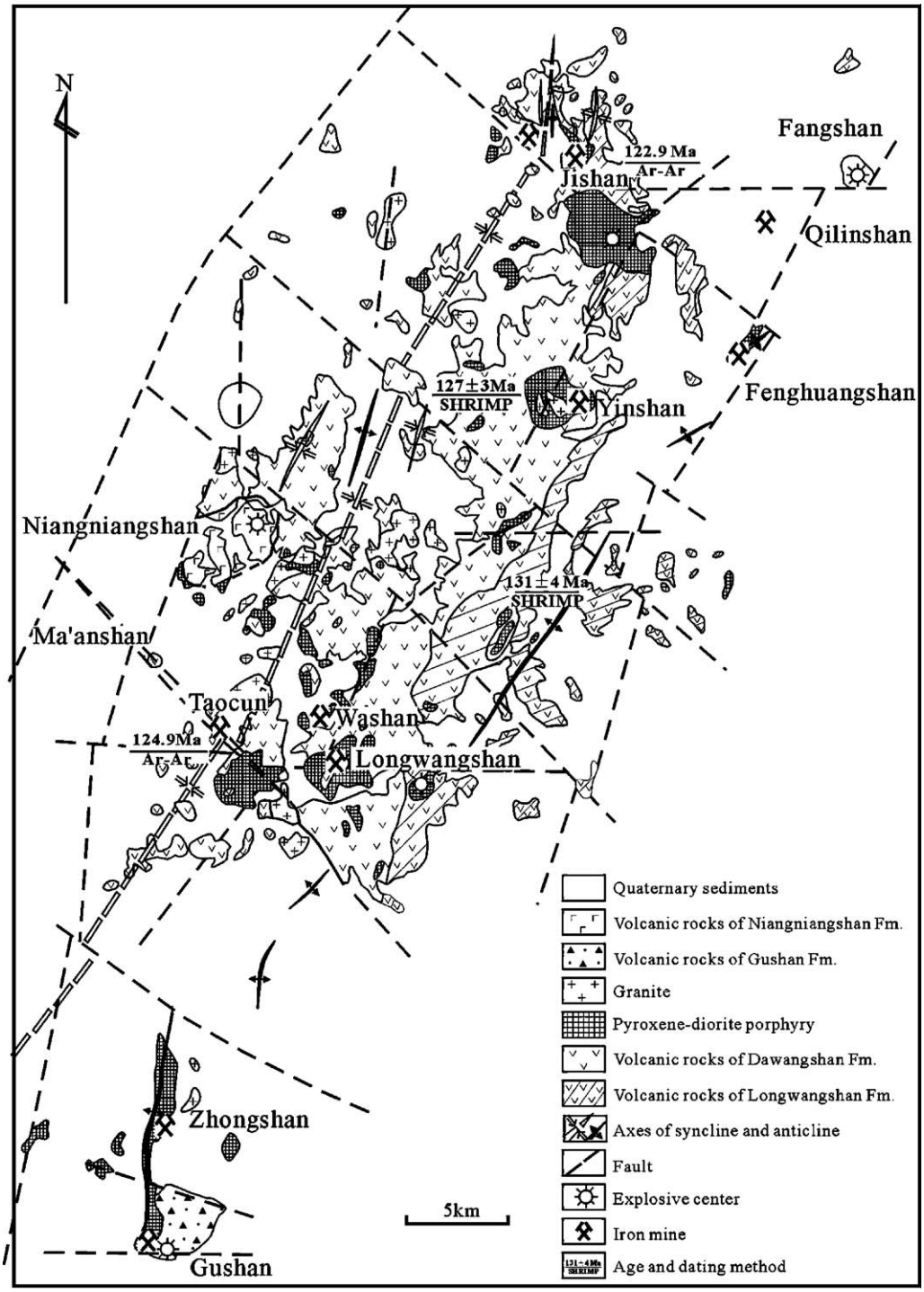

Fig. 6. Geology of the magnetite porphyry deposits in the Ningwu basin and albite sample locations. The SHRIMP zircon U–Pb data are from Zhang et al. (2003), and the albite $^{40}Ar/^{39}Ar$ age data are from Tables 3 and 4.

marialite zone, diopside–albite zone, actinolite–phlogopite–phosphorite–magnetite, and hornfels from the pyroxene diorite porphyry outward. We took two albite samples (M88-2 and t-k-2) from the albite rock alteration zone in the Meishan and Taocun iron deposits for $^{40}Ar/^{39}Ar$ dating.

4. Dating methods

4.1. Re–Os dating methods

Re–Os isotope analyses were carried out in the Re–Os Laboratory, National Research Center of Geoanalysis, Chinese Academy of Geological Sciences (CAS). Du et al. (1994, 2001), Shirey and Walker (1995), Stein et al. (2001), Markey et al. (1998), and Mao et al. (1999) have described the chemical separation procedure, which is briefly summarized here.

Enriched ^{190}Os and enriched ^{185}Re were obtained from the Oak Ridge National Laboratory. A Carius tube (a thick-walled borosilicate glass ampoule) digestion was used. The weighed sample was loaded in a Carius tube through a thin neck long funnel. The mixed ^{190}Os and ^{185}Re spike solutions and 2 ml of 12 M HCl. and 6 ml of 15 M HNO_3 were loaded while the bottom part of the tube was frozen at -80 to -50 °C in an ethanol–liquid nitrogen slush; the top was sealed using an oxygen–propane torch. The tube was then placed in a stainless-steel jacket and heated for 10 h at 230 °C. Upon cooling, the bottom part of the tube was kept frozen, the neck of the tube was broken, and the contents of the tube were poured into a distillation flask and the residue was washed out with 40 ml of water.

Os was distilled twice. In the first distillation step, OsO_4 was distilled at 105 to 110 °C for 50 min and trapped in 10 ml of water. The residual Re-bearing solution was saved in a 50-ml beaker for Re separation. The water trap solution plus 40 ml of water were distilled a second time. The OsO_4 was distilled for 1 hour and trapped in 10 ml of water that was used for ICP-MS (TJA PQ ExCell) determination of the Os isotope ratio.

The Re-bearing solution was evaporated to dryness, and 1 ml of water was added twice with heating to near-dryness in between. Ten milliliters of 20% NaOH was added to the residue followed by Re extraction with 10 ml of acetone in a 120-ml Teflon separation funnel. The water phase was then discarded and the acetone phase washed with 2 ml of 20% NaOH. The acetone phase was transferred to a 100-ml beaker that contained 2 ml of water. After evaporation to dryness, the Re was picked up in 1 ml of water that was used for the ICP-MS determination of the Re isotope ratio. Cation-exchange resin was used to remove Na if the salinity of the Re-bearing solution was more than 1 mg/ml (Du et al., 1994).

Average blanks for the total Carius tube procedure as described above were ca. 10 pg Re and ca. 1 pg Os. Analytical reliability was tested by repeated analyses of molybdenite standard HLP-5 from a carbonatite vein-type Mo–Pb deposit in the Jinduicheng-Huanglongpu area of Shanxi Province, China. Seventeen samples were analyzed over a period of 6 months. The uncertainty in each individual age determination was about 1.4% including the uncertainty of the decay constant of ^{187}Re, uncertainty in isotope ratio measurement, and spike calibrations. The average Re–Os age for HLP-5 is 221.3 ± 0.3 Ma (95% confidence limit). Median age and mean absolute deviation were 221.34 ± 0.12 Ma. The average Re concentration is 283.71 ± 1.54 μg/g. The average Os concentration is 657.95 ± 4.74 ng/g. The AIRIE Group (Colorado State University, USA) uses the same material as an in-house standard. They produced a median age of 221.30 ± 0.24 Ma on nineteen analyses run over a period of 18 months (Markey et al., 1998). The decay constant used for ^{187}Re of 1.666×10^{-11} year^{-1} has an absolute uncertainty of ± 0.017 (1.0%) (Smoliar et al., 1996).

4.2. Ar–Ar dating method

The two albite samples (M88-2 and t-k-2) taken from the Meishan and Taocun iron deposits are fresh, with the albite aggregates in paragenesis with magnetite and apatite. All measured samples were crushed and purified by magnetic separator and then cleaned by ultrasonic treatment under ethanol. The purity of the mineral separates (0.08 to 0.15 mm) exceeds 99%. Samples were wrapped by aluminum foil and loaded into an aluminum tube, together with 2 or 3 monitor samples. The tubes were sealed into a quartz bottle (40 mm high; 50 mm in diameter). The bottle was irradiated for 51 h 46 min in a nuclear reactor (The Swimming Pool Reactor, Chinese Institute of Atomic Energy, Beijing). The reactor delivers a neutron flux of $\sim 6.4 \times 10^{12}$ n cm^{-2} s^{-1}; the integrated neutron flux is about 1.21×10^{18} n cm^{-2}. After irradiation, the samples and monitors were removed from the quartz bottle and then loaded into the vacuum extraction system at the Isotopic Laboratory of the Institute of Geology and Geophysics, CAS. They were baked out for 48 h at 120 to 150 °C. The Ar extraction system comprises an electron bombardment heated furnace in which the samples are heated under vacuum. A thermocouple was used to monitor and automatically control the temperature of the furnace. The released gases are passed through a purification system. The heating-extraction step for each temperature increment was 30 min, with 30 min for purification. The purification system uses a U-tube cooled with a mixture of acetone and dry ice, and the titanium sublimation pump at 38 A filament current and

Table 1
Re–Os data of molybdenite from six Cu–Au–Mo–(Fe) ore deposits in the Middle–Lower Yangtze River valley obtained by ICP-MS analysis

Sample	Mine	Weight (g)	Re (μg/g)		^{187}Re (μg/g)		^{187}Os (ng/g)		Model age (Ma)	
			Measured	2σ	Measured	2σ	Measured	2σ	Measured	2σ
TKL-1	TKL	0.04045	53.52	0.49	33.64	0.31	78.25	0.77	139.4	2.2
TKL-2	TKL	0.04193	54.50	0.52	34.26	0.33	80.06	0.72	140.1	2.2
STJ-3	SHTJ	0.00545	674.20	6.10	423.80	3.80	975.10	8.80	138.0	2.1
STJ-4	SHTJ	0.01659	174.20	1.60	109.50	1.00	249.90	2.40	136.9	2.2
STJ-5	SHTJ	0.00157	1169.00	12.00	734.90	7.60	1736.00	20.00	141.7	2.5
NYS-1	NYSH	0.03886	53.02	0.50	33.32	0.32	77.32	0.71	139.1	2.2
NYS-4	NYSH	0.08091	29.41	0.27	18.49	0.17	42.47	0.40	137.8	2.2
NYS-5	NYSH	0.02398	184.90	1.70	116.20	1.10	265.50	2.50	136.9	2.1
YU-1	ANQ	0.03177	78.61	0.88	49.41	0.55	111.00	1.00	134.7	2.3
YU-2	ANQ	0.02813	76.95	0.73	48.37	0.46	110.80	1.10	137.4	2.2
CMS	CHMSH	0.00755	284.40	3.00	178.80	1.90	424.40	3.90	142.3	2.3
DtsZK231-1	DTSH	0.01049	261.0	2.5	164.1	1.6	380.5	2.8	139.0	2.0
DtsZK231-2	DTSH	0.01059	278.9	3.9	175.3	2.5	409.2	3.2	139.9	2.5
dtsZK231-3	DTSH	0.01065	149.8	2.2	94.2	1.4	219.3	1.8	139.6	2.6
dtsZK38151	DTSH	0.00470	754.0	15.0	474.1	9.4	1091.4	8.6	138.0	3.2
dtsZK38152	DTSH	0.01066	981.4	8.6	616.9	5.4	1427.1	11.2	138.7	2.0
dtsZK38152	DTSH	0.00113	1000.0	8.5	628.9	5.3	1476.4	11.1	140.8	2.0

Decay constant: $\lambda(^{187}\mathrm{Re}) = 1.666 \times 10^{-11}$ year^{-1} (Smoliar et al., 1996). Uncertainties are absolute at 2σ with error on Re and ^{187}Os concentrations and the uncertainty in the ^{187}Re decay constant.

a titanium sponge furnace at 800 °C. Finally, the gases were purified by two Sorb-AC pumps at room temperature. The purified argon was trapped in an activated charcoal finger at liquid–nitrogen temperature, and then released into the MM-1200B Mass Spectrometer for Ar isotope analysis.

The measured isotopic ratios were corrected for mass discrimination, atmospheric Ar contamination, blanks and irradiation-induced mass interference. The correction factors of interfering isotopes produced during irradiation were determined by analysis of irradiated pure K_2SO_4 and CaF_2. Their values are: $(^{36}Ar/^{37}Ar)_{Ca} = 0.000240$; $(^{40}Ar/^{39}Ar)_k = 0.004782$; $(^{39}Ar/^{37}Ar)_{Ca} = 0.000806$. The blanks of $m/e = 40$, $m/e = 39$, $m/e = 37$, $m/e = 36$ are less than 2×10^{-14} mol, 4×10^{-16} mol, 8×10^{-17} mol and 6×10^{-17} mol, respectively. The decay constant used is $\lambda = 5.543 \times 10^{-10}$ year^{-1}. All ^{37}Ar abundances were corrected for radiogenic decay (half-life 35.1 days). The errors are given as one standard deviation. The monitor used in this work is an internal standard: Fangshan biotite (ZBH-25) whose age is 132.7 ± 1.2 Ma and potassium content is 7.579 ± 0.030 wt.% (Wang, 1983). The $^{40}Ar/^{36}Ar$ vs. $^{39}Ar/^{36}Ar$ isochron diagram was defined by using the York regression (York, 1966, 1969).

5. Results

All 16 molybdenite samples selected were analyzed by the ICP-MS method; 9 of them were also analyzed

Table 2
Re–Os data of molybdenite from four Cu–Au–Mo–(Fe) ore deposits in the Middle–Lower Yangtze River valley obtained by NTIMS analysis

Sample	Mine	Weight (g)	Re (μg/g)		^{187}Re(μg/g)		^{187}Os (ng/g)		Model age (Ma)	
			Measured	2σ	Measured	2σ	Measured	2σ	Measured	2σ
TKL-1	TKL	0.04045	53.71	0.28	33.76	0.18	79.43	0.43	141.1	1.6
TKL-2	TKL	0.04193	54.46	0.28	34.23	0.18	82.07	0.43	143.7	1.6
STJ-3	SHTJ	0.00545	674.50	3.50	424.00	2.20	994.70	5.70	140.7	1.6
STJ-5	SHTJ	0.00157	1163.00	6.00	731.20	3.80	1742.00	10.00	142.8	1.6
NYS-1	NYSH	0.03886	52.79	0.27	33.18	0.17	77.74	0.50	140.5	1.6
NYS-4	NYSH	0.08091	29.45	0.15	18.51	0.10	43.02	0.26	139.3	1.6
NYS-5	NYSH	0.02398	184.80	1.00	116.20	0.60	272.60	1.40	140.7	1.5
YU-1	ANQ	0.03177	78.56	0.41	49.38	0.26	113.50	0.60	137.9	1.5
YU-2	ANQ	0.02813	77.32	0.40	48.60	0.25	115.60	0.80	142.6	1.7

Decay constant: $\lambda(^{187}\mathrm{Re}) = 1.666 \times 10^{-11}$ year^{-1} (Smoliar et al., 1996). Uncertainties are absolute at 2σ with error on Re and ^{187}Os concentrations and the uncertainty in the ^{187}Re decay constant.

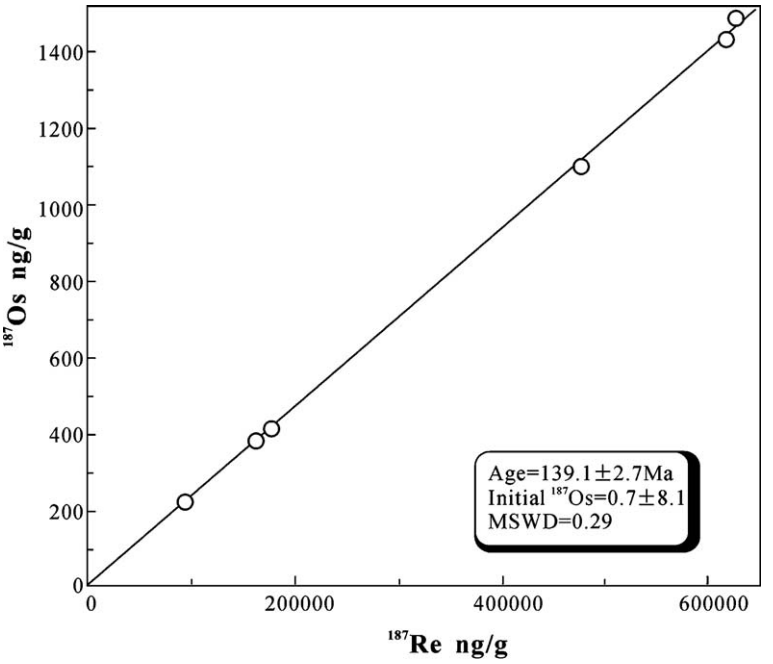

Fig. 7. Molybdenite Re–Os isochron of the Datuanshan Cu–Au–Mo deposit in the Tongling ore district, Anhui province. ISOPLOT software of Ludwig (1999) was used to calculate the isochron age, decay constant: $\lambda(^{187}\mathrm{Re}) = 1.666 \times 10^{-11}$ year^{-1} (Smoliar et al., 1996), uncertainties are absolute at 2σ.

by the NTIMS method. The data show consistency between the two methods within a small error range, even though the values generated by ICP-MS are generally lower than those of the NTIMS determination (Tables 1 and 2). The measurements on the 16 samples by the ICP-MS method yield model ages of 134.7 ± 2.3 to 142.3 ± 2.3 Ma (2σ) with an average of 138.8 ± 2.3 Ma. The model ages of the six samples from the Datuanshan stratabound Cu deposit are quite close to each other, ranging from 138.0 ± 3.2 to 140.8 ± 2.0 Ma, averaging 139.3 ± 2.6 Ma, and the isochron age calculated with the ISOPLOT software (Ludwig, 1999) is 139.1 ± 2.7 Ma (Fig. 7) with an initial Os ratio of 0.7 ± 8.1 (MSWD = 0.29). We obtained model ages of 137.9 ± 1.5 to 143.7 ± 1.6 Ma, averaging 141.0 ± 1.6 Ma by NTIMS method.

Two samples were prepared and analyzed for ^{40}Ar/^{39}Ar dating in the Isotope Laboratory of Institute of Geology and Geophysics, CAS. Detailed step-heating experiments were performed on the purified albite separates. The analytical results are listed in Tables 3 and 4 and depicted in Fig. 8. The ^{40}Ar/^{39}Ar ages presented here are reported as integrated total-gas ages (total fusion ages) of 10- and 11-step incremental heating experiments with ±1σ errors, which are generally indistinguishable from the weighted-mean pla-

Table 3
^{40}Ar/^{39}Ar dating of albite (M88-2) from the Meishan iron ore

T (°C)	$(^{40}\mathrm{Ar}/^{39}\mathrm{Ar})_m$	$(^{36}\mathrm{Ar}/^{39}\mathrm{Ar})_m$	$(^{37}\mathrm{Ar}/^{39}\mathrm{Ar})_m$	$(^{38}\mathrm{Ar}/^{39}\mathrm{Ar})_m$	$^{39}\mathrm{Ar_K} \times 10^{-12}$/mol	$(^{40}\mathrm{Ar}^*/^{39}\mathrm{Ar}) \pm 1\sigma$	$^{39}\mathrm{Ar_K}$/%	Apparent age (Ma)
400	20.247	0.0346	2.3388	0.1722	2.339	10.23 ± 0.01	1.73	173.54 ± 3.46
520	10.853	0.0219	1.6413	0.1115	3.800	4.505 ± 0.00	2.81	78.48 ± 1.12
600	10.588	0.0161	1.5888	0.0955	4.727	5.935 ± 0.00	3.50	102.68 ± 1.39
700	9.1943	0.0071	0.8461	0.0419	9.784	7.144 ± 0.00	7.24	122.91 ± 1.48
800	7.4157	0.0011	0.8332	0.0154	41.27	7.124 ± 0.00	30.5	122.57 ± 1.44
900	7.8412	0.0023	0.8676	0.0184	29.21	7.182 ± 0.00	21.6	123.54 ± 1.45
1000	8.1875	0.0036	0.8698	0.0213	22.25	7.157 ± 0.00	16.4	123.12 ± 1.45
1100	9.4791	0.0083	1.2131	0.0387	11.12	7.099 ± 0.00	8.24	122.16 ± 1.47
1200	11.886	0.0165	1.8657	0.0726	4.912	7.158 ± 0.00	3.63	123.13 ± 1.61
1300	14.768	0.0231	2.2556	0.0894	3.497	8.112 ± 0.00	2.59	138.93 ± 1.99
1450	22.500	0.0375	2.7467	0.1102	2.037	11.68 ± 0.01	1.50	196.80 ± 3.86

Sample weight = 0.1483g, J = 0.009868. Uncertainties are absolute at 1σ.

Table 4
$^{40}Ar/^{39}Ar$ dating of albite (T-K-2) from the Taocun iron ore

T (°C)	$(^{40}Ar/^{39}Ar)_m$	$(^{36}Ar/^{39}Ar)_m$	$(^{37}Ar/^{39}Ar)_m$	$(^{38}Ar/^{39}Ar)_m$	$^{39}Ar_K \times 10^{-12}$/mol	$(^{40}Ar^*/^{39}Ar) \pm 1\sigma$	$^{39}Ar_K$/%	Apparent age (Ma)
420	21.620	0.0446	2.2626	0.1396	2.073	8.640 ± .01	1.68	148.04 ± 2.26
550	12.890	0.0273	1.7958	0.1046	2.965	4.968 ± 0.00	2.41	86.61 ± 1.18
650	11.914	0.0159	1.4265	0.0829	4.357	7.313 ± 0.00	3.54	126.08 ± 1.61
750	9.0163	0.0061	0.6617	0.0381	11.31	7.234 ± 0.00	9.21	124.76 ± 1.47
850	7.8305	0.0016	0.2736	0.0182	27.37	7.324 ± 0.00	22.2	126.27 ± 1.47
950	7.5625	0.0012	0.5952	0.0240	37.10	7.214 ± 0.00	30.2	124.44 ± 1.45
1050	8.1447	0.0033	0.8296	0.0316	20.49	7.186 ± 0.00	16.6	123.96 ± 1.45
1150	9.3333	0.0072	0.8437	0.0479	11.12	7.230 ± 0.00	9.06	124.70 ± .49
1280	12.349	0.0180	2.1760	0.1054	3.845	7.189 ± 0.00	3.13	124.01 ± 1.67
1400	21.774	0.0430	2.8837	0.1666	2.153	9.344 ± 0.01	1.75	159.59 ± 2.62

Sample weight = 0.1421 g, J = 0.009868. Uncertainties are absolute at 1σ.

teau ages. The sample M88-2 from the Meishan mine yielded a 122.9 ± 0.2 Ma plateau age and a 122.6 ± 0.2 Ma isochron age. The sample t-k-2 from the Taocun iron mine yielded a 124.9 ± 0.3 Ma plateau age and a 124.9 ± 0.3 Ma isochron age.

6. Discussion and conclusions

6.1. Reliability of analytical methods and data

The measured results are mutually confirmed by the ICP-MS and NTIMS methods, and the errors are less than 2%. Meanwhile, four samples were also measured at the Re–Os Isotope Laboratory of the Colorado State University (CSU; AIRIE Program), USA, and the Chinese University of Science and Technology (CUST), China, for comparison. The age obtained from both laboratories for the sample from the Nanyangshan deposit (NYS-1) is 140.5 ± 1.6 Ma (CUST) vs. 141.1 ± 0.5 Ma (CSU): The sample from the Tongkuangli deposit (TKL-2) gave 143.7 ± 1.6 Ma (CUST) vs. 143.6 ± 0.5 Ma (CSU), and the sample from the Anqing Cu–Mo deposit (YU-1) gave 137.9 ± 1.5 Ma (CUST) vs. 139.1 ± 0.4 Ma (CSU). The data show that the two analytical methods from three different laboratories are consistent, indicating that the data we obtained in this

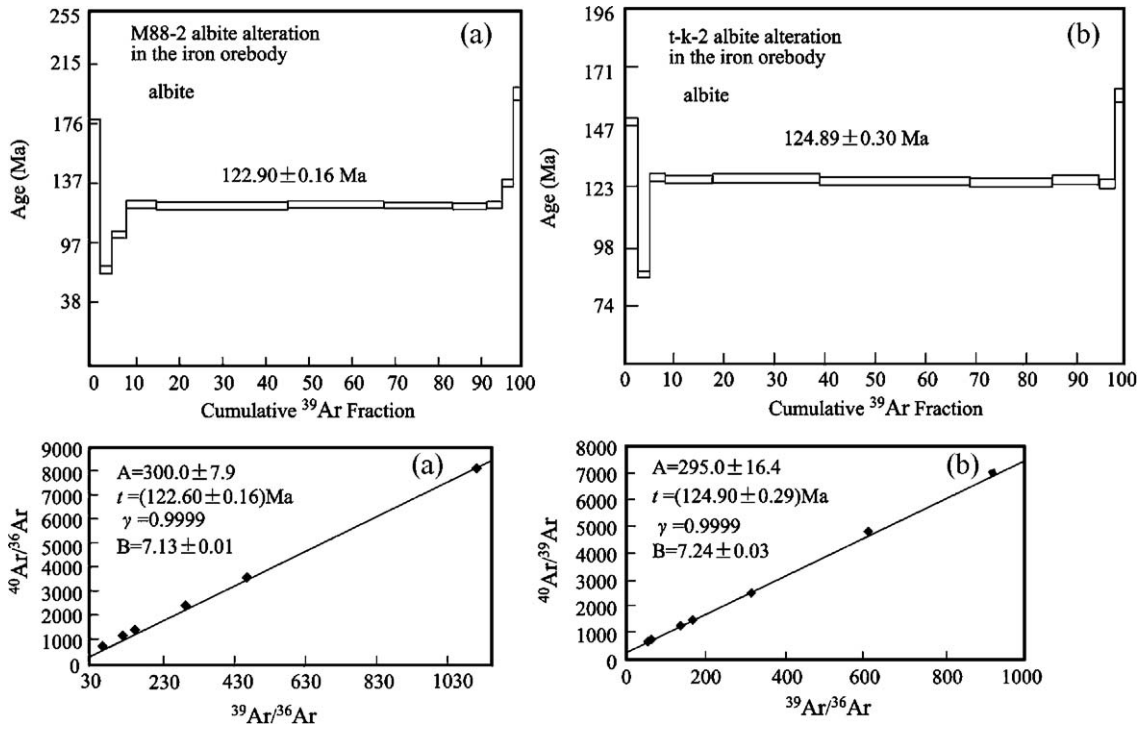

Fig. 8. Plateau and isochron $^{40}Ar/^{39}Ar$ ages of albite from the Meishan (a) and Taocun (b) magnetite porphyry deposits in the Ningwu basin.

study are both precise and reliable. Our data are also quite close to the Os–Os and Re–Os data obtained by Sun et al. (2003). They reported an Os–Os model age of 138.0 ± 2.5 Ma and a Re–Os model age of 139.02 ± 0.34 Ma for the Longhushan deposit, which belongs to the Shizishan ore district which also comprises the Datuanshan deposit. The Tongniujing deposit, from the same ore field as the Anqing mine, gave an Os–Os model age of 136.1 ± 2.0 Ma. Furthermore, our data are also quite close to the biotite $^{40}Ar/^{39}Ar$ ages of 139.8 to 135.8 Ma of the related granitic stock (Wu et al., 1996).

6.2. Ore genesis of porphyry/skarn/stratabound Cu–Au–Mo–(Fe) deposits

Zhai et al. (1992) summarized, in detail, the mineralization and metallogenic associations in the Middle–Lower Yangtze River valley, based on the body of K–Ar and Rb–Sr data generated in the 1980s. They suggest that the time of the Yanshanian mineralization in the belt extends from 170 to 90 Ma, with the Cu–Mo–Au–(Fe) deposits emplaced at 160 to 120 Ma, and the magnetite porphyry deposits at 130 to 90 Ma. The data obtained in this study show that the metallogenic timing of Cu–Mo–Au–(Fe) deposits in the Middle–Lower Yangtze River valley ranges from 134.7 ± 2.2 to 143.7 ± 1.6 Ma. The albite $^{40}Ar/^{39}Ar$ ages of the Ningwu magnetite porphyry deposits are 122.9 ± 0.2 to 124.9 ± 0.3 Ma, indicating that they developed in the Ningwu-Luzhong volcanic basins later than the Cu–Mo–Au–(Fe) deposit. In addition, the SHRIMP zircon U–Pb ages of volcanic rocks of the Dawangshan and Longwangshan Formations are 127 ± 3 and 131 ± 4 Ma, respectively (Zhang et al., 2003), indicating that the volcanic rocks are temporally related to the magnetite porphyry mineralization, and later than the Cu–Mo–Au mineralization and related granitoid intrusions. All these data suggest that the Ningwu-Luzhong volcanic basins resulted from extension subsequent to porphyry/skarn/manto Cu–Mo–Au mineralization.

In the Middle–Lower Yangtze River metallogenic belt, there are various types of Cu–Au–Mo–(Fe) deposits: skarn deposits (e.g., Tongkuangli Mo, Shatanjiao and Nanyangshan Cu–Mo–Au deposits); porphyry-only deposits (e.g., Shaxi porphyry Cu–Au deposit; Xu et al., 1999), and in some deposits, such as Chengmenshan and the Dongguashan, skarn and porphyry mineralization developed simultaneously (Tang et al., 1998). Moreover, there also exist a number of bedded skarn and/or bedded massive sulfide orebodies. All the Cu–Au orebodies occur in carbonate strata of Carboniferous, Permian, and Triassic age, the so-called “three beds structure” in the model of Zhai et al. (1992). Although the bedded orebodies are extensively developed along the Carboniferous, Permian, and Triassic carbonate layers, the most important stratabound orebodies occur dominantly at the unconformity between the Devonian Wutong Formation siltstone and shale and the Carboniferous Gaolishan Formation limestone or dolomite of the Upper Carboniferous Huanglong Formation. The Dongguashan deposit (Shizishan ore district), and several orebodies in the Xinqiao ore district are good examples. Because of their morphologies and features suggestive of a syngenetic sedimentary and/or replacement genesis, some researchers suggested they were the consequence of submarine exhalative sedimentary processes (Fu, 1977; Gu, 1984; Ji and Wang, 1990; Yue et al., 1993), and formed in Variscan to Indosinian times. Other researchers, however, have argued against such a proposal. Compared with many deposits in North America, including the world-class Bingham Cu deposit, Pan and Dong (1999) suggest that porphyry/skarn/manto orebodies in the Middle–Lower Yangtze River valley are the products of the same metallogenic system as the deposits related to Yanshanian granitoids. The major problem for the exhalative sedimentary model is that these Cu–Mo–Au and S–Fe–(Cu) orebodies occur along the unconformity. Determinations of Cu isotopes in chalcopyrite from the stratabound Cu–Au–Mo orebody in the Dongguashan deposit in Tongling ore field indicate that the Cu is derived from the Yanshanian granitic magma system (Lu et al., 2003). Sulfur and Pb isotopes in the ores are similar to the granitoids although they display mixing with some lead and sulfur from the sedimentary rocks (Pan and Dong, 1999).

Zang et al. (2004) have given a detailed geological observations on the Xinqiao Cu–Au deposit with implications for ore genesis. They suggest that, except for the siderite layers which could be a result of the sedimentary process of littoral facies, the massive sulfide ores developed along the unconformable boundary between Devonian sandstone and Middle Carboniferous carbonate rocks, with clear features of epigenetic mineralization. Based on the characteristics described above, Chang and Liu (1983), Chang et al. (1991), Zhai (1992), Zhai et al. (1992, 1996), and Tang et al. (1998) proposed that magmatic fluids are predominant in the Yanshanian metallogenic process, while some syngenetic sedimentary components could have been incorporated in the metallogenic system. According to their studies on the Xinqiao deposit (Tongling area), Xu and Zhou (2001) also suggest that the mineralization resulted from reactivation of

sulfides in the Carboniferous strata by the Yanshanian granitic fluids.

The precise data for the bedded orebody in the stratabound Datuanshan deposit we have obtained in this study show that the ages of Cu–Mo–Au sulfides are 138.0 ± 3.2 to 140.8 ± 2.0 Ma, with an average of 139.3 ± 2.6 Ma. Furthermore, the initial Os ratio of 0.7 ± 8.1 (MSWD = 0.29) indicates that there is almost no common Os involved in the isotopic system during mineralization, and almost all Os is of radiogenic origin. This is in sharp contrast to the 40% to 50% common Os in the Mo–Ni ore layer hosted in black shale at the bottom of the Cambrian system in the Huangjiawan deposit, Guizhou province—a typical deposit related to submarine exhalative sedimentary or 'normal' sedimentary processes (Horan et al., 1994; Mao et al., 2002). All this information implies that the stratabound orebodies are the result of replacement and not submarine exhalative sedimentation.

The Re contents of the 16 samples range from 29 to 1000 ppm. Mao et al. (1999, 2003a) and Stein et al. (2001) have summarized how the Re content of molybdenite can be used to trace the source of the ore-forming materials. Absolute abundances decrease from deposits related to a mantle source to those related to I-type and S-type granites. The high Re content of molybdenites from the Middle–Lower Yangtze River valley indicates that the granitic stocks related to the Cu–Mo–Au–Fe mineralization are derived from crust–mantle anatexis. Deng et al. (1999) suggested that the extensive crust–mantle interaction is a possible setting for rock- and ore-forming processes in the Middle–Lower Yangtze River valley during the Late Cretaceous.

6.3. Geodynamic environment and model for the mineralization

The Middle–Lower Yangtze River metallogenic belt is located in the northern margin of the Yangtze craton, but its geodynamic evolution is similar to that of the North China craton (Mao et al., 2003b). There are three periods of large-scale mineralization of Mesozoic age in the North China craton and its adjacent areas (190 to 160, ~140, and 115 to 125 Ma). The corresponding geodynamic settings are post-collisional orogeny, transformation of the tectonic regimes, and large-scale delamination of the lithosphere (Mao et al., 2003b). Obviously, the two periods of the porphyry/skarn/stratabound Cu–Mo–Au–(Fe) ore formation related to granitic rocks and the porphyry Fe deposits related to terrestrial subvolcanic rocks in the Middle–Lower Yangtze River valley are consistent with the latter two geodynamic settings in the North China craton.

The comprehensive study of Chang et al. (1991) indicated that the Middle–Lower Yangtze River valley developed on Precambrian basement of Late Proterozoic age and remained quite stable during the Paleozoic as a wide open trough with vertical movements. From the Cambrian to the Early Triassic, the Middle–Lower Yangtze River valley represented a stable trough filled by carbonate and clastic rocks of shallow marine facies (Xu, 1985). Collision between the Yangtze and North China cratons took place at 238–218 Ma (Li et al., 1989, 1997; Ames et al., 1993, 1996; Chen et al., 1995; Chavagnac and Jahn, 1996; Rowley et al., 1997; Li, 2001). From the Middle Triassic to the Middle Jurassic, this belt was a foreland basin located south of the Dabie Orogen, which is composed by a series of depressions filled with a suite of clastic rocks, and the lake-facies sedimentary rocks of the Middle Jurassic Luoling Formation (Tang et al., 1998). During this period, geodynamics are characterized by extension and thinning of the lithosphere and mantle uplift (Fig. 9a). Ren et al. (1998), Mao et al. (2003b), and Niu et al. (2003) suggested that the NS-trending principal stress field changed progressively to an EW-trending principal stress field from 160 to 135 Ma in the eastern China continent, due to the convergence of the Paleo-Pacific and Euroasian Plates. The Cu–Mo–Au–(Fe) metallogenic system in the Middle–Lower Yangtze River valley formed at the end of this period of geodynamic adjustment, and is the second pulse of Mesozoic large-scale mineralization (Mao et al., 2003b). The granitic magma related to mineralization resulted from anatexis of the magma from both lower crust and upper mantle with diapiric emplacement. Due to intense crust–mantle interaction, there exist many enclaves of mantle rock and giant crystals of hornblende in the granitoid intrusions (Du and Li, 1997; Qin et al., 2002). In this period, the Middle–Lower Yangtze River valley experienced mantle uplift. The orebodies and related granitic intrusions were emplaced at the intersections of EW- and NNE-trending faults (Fig. 9b). After geodynamic adjustment, an extensional regime developed in the EW-trending principal stress field possibly caused by lithospheric delamination or "lithosphere–asthenosphere catastrophe" (Deng et al., 1999). As part of the East China continent, rapid extension and dramatic thinning of the lithosphere occurred in the Middle–Lower Yangtze River valley along with development of a series of parallel NNE-trending fault basins and

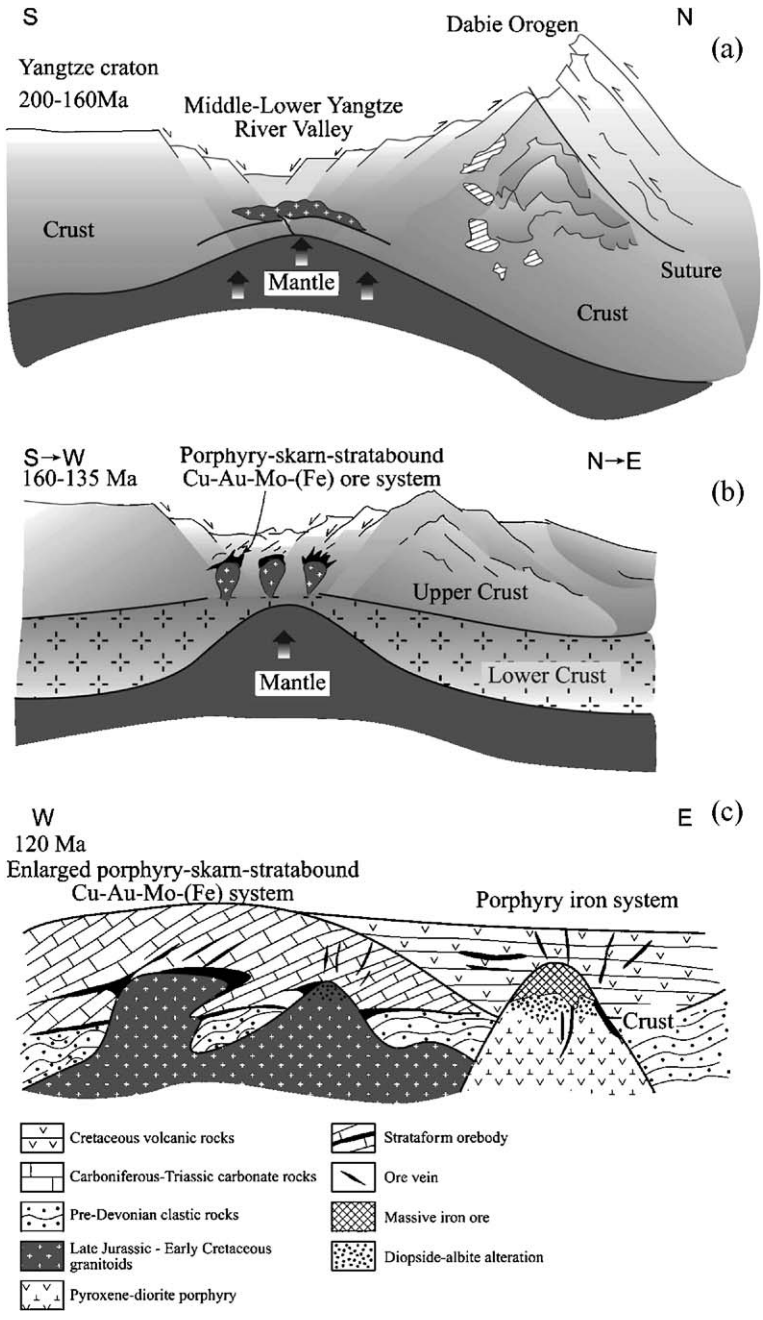

Fig. 9. Geodynamic model for ore formation in the Middle–Lower Yangtze River valley metallogenic belt in East China. (a) Foreland basin evolution stage with mantle underplating during post-collision period (220–160 Ma). (b) Transition period of regional geodynamic principal stress field from NS- to near EW-trending (160–135 Ma), which was accompanied by intrusion of I-type granitoids at shallow level and related porphyry–skarn–manto Cu–Au–Mo mineralization (around 140 Ma). (c) Dramatic thinning of Cretaceous lithosphere, accompanied by andesitic magma eruption and related magnetite porphyry mineralization (131–123 Ma), which is connected to lithospheric delamination.

intense volcanism at 125 to 115 Ma. The latter caused formation of the magnetite porphyry systems associated with Cretaceous andesitic volcanic and subvolcanic rocks in the Ningwu-Luzhong volcanic fault basins (Fig. 9c).

Acknowledgements

We thank Chu Guozheng, Du Jianguo and Zhang Chenghuo from the Anhui Geological Survey, and the Jiangxi Bureau of Mineral Resources and Exploration

for their kind support and help during the field investigation. We greatly appreciate the constructive discussions with Chen Yuchuan, Pei Rongfu, Chang Yinfo, Zhai Yusheng, Zhao Yiming, Wu Ganguo, Dong Shuwen, Deng Jun, Du Yangsong, Chen Jiangfeng, Xu Zhigang, Shunso Ishihara, Rod Kirkham, Richard J. Goldfarb, Feng Rui, Pan Yuanming, Qu Wenjun, Yang Gang, Meng Yifeng, and Zeng Pusheng. We are also grateful to the two anonymous reviewers who provided many constructive suggestions. This study was financially supported by the Major State Basic Research Program (G1999043216, G1999043211), National Natural Science Fund of China (No. 40434011) and the Large-scale Geological Survey Project (K1.4). This paper is also a contribution to IGCP project 473.

References

Ames, L., Tilton, G.R., Zhou, G., 1993. Timing of collision of the Sino-Korean and Yangtse cratons: U–Pb zircon dating of coesite-bearing eclogites. Geology 21, 339–342.

Ames, L., Zhou, G., Xiong, B., 1996. Geochronology and isotopic character of ultrahigh-pressure metamorphism with implications for collision of the Sino-Korean cratons, central China. Tectonics 15, 472–489.

Chang, Y.F., Liu, X.G., 1983. On stratabound skarn deposits. Mineral Deposits 2, 11–20 (in Chinese).

Chang, Y.F., Liu, X.P., Wu, C.Y., 1991. The copper–iron belt of the Lower and Middle Reaches of the Changjiang River. Geological Publishing House, Beijing. 234 pp. (in Chinese).

Chavagnac, N.O., Jahn, B., 1996. Coesite-bearing eclogites from the Bixiling complex, Dabie mountains, China: Sm–Nd ages, geochemical characteristics and tectonic implication. Chemical Geology 133, 29–51.

Chen, J., Xie, Z., Liu, S., Li, X., Foland, K.A., 1995. Cooling age of Dabie orogen, China, determined by ^{40}Ar–^{39}Ar and fission track techniques. Science in China. Series B, Chemistry, Life Sciences & Earth Sciences 38, 749–757.

Deng, J.F., Mo, X.X., Zhao, H.L., Luo, Z.H., Zhao, G.C., Dai, S.Q., 1999. The Yanshanian lithosphere–asthenosphere catastrophe and metallogenic environment in East China. Mineral Deposits 18, 309–315 (in Chinese with English abstract).

Du, Y.S., Li, X.J., 1997. Enclaves in the typical mining districts of Tongling, Anhui and their implication to the process of magmatism-metallogeny. Geological Journal of China Universities 3, 171–182 (in Chinese with English abstract).

Du, A.D., He, H.L., Yin, N.W., Zou, X.Q., Sun, Y.L., Sun, D.Z., Chen, S.Z., Qu, W.J., 1994. A study on the rhenium–osmium geochronometry of molybdenites. Acta Geologica Sinica 68, 339–347.

Du, A.D., Zhao, D.M., Wang, S.X., 2001. Precise Re–Os dating for molybdenite by ID-NTIMS with tube sample preparation. Rock and Mineral Analysis 20, 247–252 (in Chinese with English abstract).

Du, Y.S., Tian, S.H., Li, X.J., Lee, H.K., 2003. Contrast in fluid metallogeny between the Tianmashan Au–S deposit and the Datuanshan Cu deposit in Tongling, Anhui province. Acta Geologica Sinica 77, 116–124.

Fu, S.G., 1977. Geological characteristics of the copper deposits of the submarine eruption-sedimentary type in Middle Carboniferous in the Middle–Lower Yangtze River metallogenic belt. Journal of Nanjing University. Natural Science Edition 1, 43–62 (in Chinese with English abstract).

Gu, L.X., 1984. Middle Carboniferous submarine volcanic rocks and massive sulfide deposits in Wushan, Jiangxi Province. Journal of Guilin College of Geology 4, 91–102 (in Chinese with English abstract).

Gu, L.X., Xu, K.Q., 1986. On the Middle Carboniferous submarine massive sulfide deposits in the Middle–Lower Yangtze River region. Acta Geologica Sinica 60, 176–186.

Guo, W.K., 1957. On the genesis of the Tongguanshan copper deposit. Acta Geologica Sinica 37, 317–332.

Guo, Z.S., 1957. Some skarn copper deposits in Lower Yangtze River valley. Acta Geologica Sinica 37, 1–10.

Guo, W.K., 1963. Original zoning of some metallic deposit and its genesis. Acta Geologica Sinica 43, 247–270.

Guo, W.K., 1982. On the granitoids and metal mineralization. Regional Geology of China 2, 15–30 (in Chinese with English abstract).

Horan, M.F., Morgan, J.W., Grauch, R.I., Coveney Jr., R.M., Murowchick, J.B., Hulbert, L.J., 1994. Rhenium and osmium isotopes in black shales and Ni–Mo–PGE-rich sulfide layers, Yukon Territory, Canada, and Hunan and Guizhou provinces, China. Geochimica et Cosmochimica Acta 58, 257–265.

Hu, S.X., Zhou, S.Z., Sun, Z.M., Ren, Q.J., 1979. On the metallogenic specialization of the intermediate-acid rocks related to Fe, Cu deposits in the eastern China. Acta Geologica Sinica 53, 323–336.

Huang, X.C., Chu, G.Z., 1993. Metallogenic model of the ore deposits in the Shizishan orefield, Tongling. Mineral Deposits 12, 213–221 (in Chinese with English abstract).

Ishihara, S., 1977. The magnetite-series and ilmenite-series granitic rocks. Mining Geology 27, 293–305.

Ji, S.X., Wang, W.B., 1990. Copper Deposits in Northwestern Jiangxi. Geological Publishing House, Beijing. 253 pp. (in Chinese).

Li, J.Y., 2001. Timing and pattern of collision of the Sino-Korea and Yangtze cratons: the evolution of the Sinian-Jurassic sedimentary environment in the Middle–Lower Reaches of Yangtze River. Acta Geologica Sinica 75, 25–34.

Li, S.G., Ge, G.J., Liu, D.L., Zhang, Z.Q., Ye, X.J., Zheng, S.G., Peng, C.Q., 1989. Sm–Nd isotopic ages of the C-type eclogite from the Dabie group in the north Dabieshan area and its significance. Chinese Science Bulletin 34, 522–525.

Li, S.G., Li, H.M., Chen, Y.Z., 1997. Chronology of the ultrahigh-pressure metamorphic rocks in the Dabieshan-Sulu area: zircon U–Pb isotopic systematics. Science in China (Series D) 27, 310–322.

Liu, X.P., Chang, Y.F., Wu, C.Y., 1988. On the metallogenic conditions and metallogeny of the Middle–Lower Yangtze River region. Acta Geologica Sinica 62, 167–177.

Lu, J.J., Hua, R.M., Jiang, S.Y., 2003. Copper isotope study of copper and gold deposit of Dongguashan, China. Geochimica et Cosmochimica Acta 67 (18S), A260.

Ludwig, K., 1999. Isoplot/Ex, version 2.0: A Geochronological Toolkit for Microsoft Excel. Special Publication, vol. 1a. Geochronology Center, Berkeley.

Mao, J.W., Zhang, Z.C., Zhang, Z.H., Du, A.D., 1999. Rhenium–osmium isotopic dating of molybdenite in the Xiaoliugou W (Mo) deposit in North Qilian Mountains and its geological significance. Geochimica et Cosmochimica Acta 63, 1815–1818.

Mao, J.W., Lehmann, B., Du, A.D., Zhang, G., Ma, D., Wang, Y., Zeng, M., Kerrich, R., 2002. Re–Os dating of polymetallic Ni–Mo–PGE–Au mineralization in lower Cambrian black shales of south China and its geological significance. Economic Geology 97, 1051–1061.

Mao, J.W., Du, A.D., Seltmann, R., Yu, J.J., 2003a. Re–Os dating for the Shameika porphyry Mo deposit and the Lipovy Log pegmatite rare metal deposit in the central and southern Urals. Mineralium Deposita 38, 251–257.

Mao, J.W., Wang, Y.T., Zhang, Z.H., Yu, J.J., Niu, B.G., 2003b. Geodynamic settings of Mesozoic large-scale mineralization in the North China and adjacent areas: implication from the highly precise and accurate ages of metal deposits. Science in China (Series D) 33, 838–851.

Markey, R., Stein, H., Morgan, J., 1998. Highly precise Re–Os dating for molybdenite using alkaline fusion and NTIMS. Talanta 45, 935–946.

Mei, Y.X., Mao, J.W., Li, J.W., Du, A.D., 2005. Re–Os dating of molybdenite from strataform skarn orebodies in the Datuanshan copper deposit, Tongling, Anhui province, and its geological significance. Acta Geoscientia Sinica 26, 327–331 (in Chinese with English abstract).

Ningwu Research Group, 1978. Magnetite Porphyry Deposits in Ningwu area. Geological Publishing House, Beijing. 196 pp. (in Chinese).

Niu, B.G., He, Z.J., Song, B., Ren, J.S., 2003. SHRIMP dating of the Zhangjiakou volcanic series and its significance. Geological Bulletin of China 22, 140–141 (in Chinese with English abstract).

Pan, Y., Dong, P., 1999. The Lower Changjiang (Yangzi/Yangtze River) metallogenic belt, East China: intrusion- and wall rock-hosted Cu–Fe–Au, Mo, Zn, Pb, Ag deposits. Ore Geology Reviews 15, 177–242.

Pei, R.F., Hong, D.W., 1995. The granites of South China and their metallogeny. Episodes 18, 77–86.

Qin, X.L., Du, Y.S., Tian, S.H., Lee, X.J., Yin, J.W., Jin, S.Z., 2002. First discovery of the pyrrhotite–chalcopyrite-bearing amphibole megacrysts in Tongling, Anhui Province. Advance in Natural Sciences 12, 834–838 (in Chinese with English abstract).

Ren, J.S., Niu, B.G., He, Z.J., Xie, G.L., Liu, Z.G., 1998. Tectonic pattern and dynamic evolution of the East China. In: Jishun, Ren, Weiran, Yang (Eds.), The Lithosphere Structure and Tectono-Magma Evolution of the East China. Seismology Press, pp. 1–12 (in Chinese with English abstract).

Rowley, D.B., Xue, F., Turker, R.D., Peng, Z.X., Baker, J., Davis, A., 1997. Age of ultrahigh pressure metamorphism and protolith of orthogneisses from the eastern Dabie Shan: U/Pb zircon geochemistry. Earth and Planetary Science Letters 151, 191–203.

Shirey, S.B., Walker, R.J., 1995. Carius tube digestion for low-blank rhenium–osmium analysis. Analytical Chemistry 67, 2136–2141.

Smoliar, M.I., Walker, R.J., Morgan, J.W., 1996. Re–Os ages of group IIA, IIIA, IVA and VIB iron meteorites. Science 271, 1099–1102.

Stein, H.J., Markey, R.J., Morgan, J.W., Hannah, J.L., Schersten, A., 2001. The remarkable Re–Os chronometer in molybdenite: how and why it works. Terra Nova 13, 479–486.

Sun, W., Xie, Z., Chen, J., Zhang, X., Chai, Z., Du, A., Zhao, J., Zhang, C., Zhou, T., 2003. Os–Os dating of copper and molybdenum deposits along the Middle and Lower reaches of the Yangtze river, China. Economic Geology 98, 175–180.

Tang, Y.C., Wu, C.Y., Chu, G.Z., Xing, F.M., Wang, Y.M., Cao, F.Y., Chang, Y.F., 1998. Geology of copper–gold polymetallic deposits in the along-Changjiang area of Anhui province. Geological Publishing House, Beijing. 351 pp. (in Chinese with English abstract).

Wang, S.S., 1983. Dating of the Chinese K–Ar standard sample (Fangshan biotite, ZBH-25) by using the $^{40}Ar/^{39}Ar$ method. Scientia Geologica Sinica 4, 315–321 (in Chinese with English abstract).

Wang, D.Z., Ren, Q.J., Qiu, J.S., Chen, K.R., Xu, Z.W., Zeng, J.H., 1996. Characteristics of volcanic rocks in the shoshonite province, eastern China, and their metallogenesis. Acta Geologica Sinica 70, 23–34.

Wang, Q., Zhao, Z.H., Xiong, X.L., Xu, J.F., 2001. Melting of the underplated basaltic lower crust: evidence from the Shaxi adakitic sodic quartz diorite–pophyrites, Anhui Province, China. Chinese Journal of Geochemistry 30, 353–362.

Wu, L.S., Wu, Z.Z., 1999. Two Mesozoic tectonic events in Jiurui area, Jiangxi province and their controlling roles on rock-forming and ore-forming activities. Mineral Deposits 18, 129–137 (in Chinese with English abstract).

Wu, C.L., Zhou, X.R., Huang, X.C., Zhang, C.H., Huang, W.M., 1996. $^{40}Ar/^{39}Ar$ chronology of intrusive rocks from Tongling. Acta Petrologica et Mineralogica 15, 299–307 (in Chinese with English abstract).

Wu, G.G., Zhang, D., Zang, W.S., 2003. Study of tectonic layering motion and layering mineralization in the Tongling metallogenic cluster. Science in China (Series D) 33, 8852–8863.

Xu, Z.G., 1985. Genesis of Mesozoic volcanic rocks in eastern China as discussed in light of the characteristics of the structural stress field. Acta Geologica Sinica 59, 109–126 (in Chinese with English abstract).

Xu, G., Zhou, J., 2001. The Xinqiao Cu–S–Fe–Au deposit in the Tongling mineral district, China: synorogenetic remobilization of a stratiform sulfide deposit. Ore Geology Reviews 18, 77–94.

Xu, W.Y., Xu, Z.W., Gu, L.X., Ren, Q.J., Fu, B., Niu, C.W., 1999. Heat evolution from intrusion to mineralization in Shaxi porphyry copper (gold) deposits, Anhui Province. Geological Review 45, 361–367 (in Chinese with English abstract).

York, D., 1966. Least squares fitting of a straight line. Canadian Journal of Physics 44, 1079–1086.

York, D., 1969. Least squares fitting of a straight line with correlated errors. Earth and Planetary Science Letters 5, 320–324.

Yue, W.Z., Ye, Z.Z., Wei, N.Y., Jiang, Y.H., Ji, S.X., 1993. Sedimentary geology and stratabound massive deposits of Late Carboniferous age in the Middle and Lower Yangtze Reaches. Geological Publishing House, Beijing. 159 pp. (in Chinese with English abstract).

Zang, W.S., Wu, G.G., Zhang, D., Li, J.W., Liu, A.H., Zhang, Z.Y., 2004. Preliminary study on the Xinqiao S–Fe ore field: some geological evidences. Acta Geologica Sinica 77, 548–557.

Zhai, Y.S., 1992. Metallogenic regularities of iron–copper (gold) deposits in Middle–Lower Yangtze River valley. Geological Publishing House, Beijing. 235 pp.

Zhai, Y.S., Yao, S.Z., Lin, X.D., 1992. Metallogeny of iron and copper deposits in the Middle–Lower Yangtze River region. Mineral Deposits 11, 1–12 (in Chinese with English abstract).

Zhai, Y.S., Xiong, Y.Y., Yao, S.Z., Liu, X.D., 1996. Metallogeny of copper and iron deposits in the Eastern Yangtze Craton, east-central China. Ore Geology Reviews 11, 229–248.

Zhang, Q., Wang, Y., Qian, Q., Yang, J.H., Wang, Y.L., Zhao, T.P., Guo, Z.H., 2001. The characteristics and tectonic–metallogenic significances of the adakites in Yanshan period from eastern China. Acta Petrologica Sinica 17, 236–244 (in Chinese with English abstract).

Zhang, Q., Jian, P., Liu, D.Y., Wang, Y.L., Qian, Q., Xue, H.M., 2003. SHRIMP dating of volcanic rocks from Ningwu area and geological implication. Science in China (Series D) 33, 830–837 (in Chinese with English abstract).

Zhao, Y.M., Lin, W.W., Bi, C.S., Li, D.X., Jiang, C.J., 1990. Skarn Deposits of China. Geological Publishing House, Beijing. 354 pp. (in Chinese with English abstract).

Zhao, Y.M., Zhang, Y.N., Bi, C.S., 1999. Geology of gold-bearing skarn deposits in the Middle and Lower Yangtze River Valley and adjacent regions. Ore Geology Reviews 14, 227–240.

Zhou, T.F., Yuan, F., Yue, S.C., Liu, X.D., Zhao, Y., 2002. Water/rock interaction during formation of skarn-type deposits in Yueshan orefield, Anhui province. Mineral Deposits 21, 1–9 (in Chinese with English abstract).